Size Dependence of Tracer Diffusion in a Laponite Colloidal Gel

Laure Petit, Catherine Barentin, Jean Colombani, Christophe Ybert, Lydéric Bocquet

▶ **To cite this version:**

Laure Petit, Catherine Barentin, Jean Colombani, Christophe Ybert, Lydéric Bocquet. Size Dependence of Tracer Diffusion in a Laponite Colloidal Gel. Langmuir, 2009, 25 (20), pp.12048 - 12055. 10.1021/la901244v . hal-01628770

HAL Id: hal-01628770
https://hal.science/hal-01628770

Submitted on 17 May 2022

HAL is a multi-disciplinary open access archive for the deposit and dissemination of scientific research documents, whether they are published or not. The documents may come from teaching and research institutions in France or abroad, or from public or private research centers.

L'archive ouverte pluridisciplinaire **HAL**, est destinée au dépôt et à la diffusion de documents scientifiques de niveau recherche, publiés ou non, émanant des établissements d'enseignement et de recherche français ou étrangers, des laboratoires publics ou privés.

Size dependence of tracer diffusion in a Laponite colloidal gel

Laure Petit, Catherine Barentin,* Jean Colombani, Christophe Ybert, and Lydéric Bocquet

Laboratoire de Physique de la Matière Condensée et Nanostructures ; Université de Lyon ; Université Claude Bernard Lyon 1;

CNRS, UMR 5586, Domaine scientifique de la Doua, F-69622 Villeurbanne Cedex, France

E-mail: barentin@lpmcn.univ-lyon1.fr

Abstract

Using a Fluorescence Recovery After Photobleaching (FRAP) technique, we present measurements of probe diffusion in a colloidal glass –a Laponite suspension. By varying the probe size over two orders of magnitudes, as well as the concentration of the colloidal glass, we evidence and quantify the deviations of the probe diffusivity from the bulk Stokes–Einstein expectations. These experiments suggest that the probe diffusion in the dynamically arrested Laponite structure is mainly controlled by the ratio between the probe size and the typical clay platelets inter-distance. Comparing with a simple hindered diffusion mechanism, the reduction of tracer diffusion is discussed in terms of the hydrodynamic interaction of the probe with the Laponite structure. Finally these results can be interpreted in terms of a scale dependent viscosity of the colloidal glass.

Introduction

Soft glassy materials – as exemplified by concentrated emulsions, granular materials, colloidal glasses, etc. – are complex and disordered materials encountered in a wide range of every day life applications, from paints to cosmetics or food industry.[1,2] The description of these systems, the behavior of which is intermediate between solid and fluid, is however fundamentally challenging due to their intrinsic out-of-equilibrium nature, associated with the dynamical arrest in disordered state occurring at the jamming (or glass) transition.[3]

As such, the understanding of the complex phenomenology shared by these diverse systems has attracted numerous theoretical and experimental works devoted in particular to the breakdown of ergodicity and the existence of long relaxation times leading to the so-called aging of the material, the identification of dynamical heterogeneities in the material between 'frozen' and fast relaxing regions,[4,5] or the appearance of a strongly heterogeneous material response under flow and deformation associated with shear-banding phenomena and flow cooperativity.[6–8]

Among the various systems studied so far, aqueous suspension of Laponite clay platelets have been used extensively due to its industrial interest as gelling agent or oil drilling fluid, together with practical advantages associated with its transparency – which makes it well suited for light scattering or other optical techniques – and the fact that it exhibits a complete phenomenological picture, from aging to shear-thinning, thixotropy and shear-banding. Laponite suspensions in their glassy state were used for instance to study aging dynamics associated with slow structural relaxation due to cooperative reorganizations of particles[9,10] in soft glassy materials. They were used also to investigate the theoretical proposal of extending the well-known fluctuation-dissipation theorem formalism to describe out-of-equilibrium systems, through the incorporation of an effective temperature $T_{\text{eff.}}$ differing from the bath temperature.[11–15] One should however acknowledge that the origin of the dynamical arrest in Laponite suspension remains debated: whether the solidification of the material stems from the attraction between the negatively charged faces and positively charged edges of Laponite platelets, providing percolating aggregates as in gels, or from the repulsion between the electrical double layers of the Laponite platelets, as in glasses, has not received a

general agreement.[10,16–18]

Overall, this points to the difficulties inherent to the description of these soft glassy materials and to the need for additional information on the local dynamical properties in such systems. This is the purpose of the present work where the Laponite suspension behavior and structure is probed through the measurement of the diffusive properties of colloidal tracer particles of various sizes. The diffusive motion of particles in simple liquids is well described by the celebrated Stokes-Einstein relation:

$$D = \frac{kT}{\xi} \tag{1}$$

where $\xi = 3\pi\eta\sigma$ is the Stokes friction coefficient for a sphere with diameter σ; η is the viscosity of the simple liquid considered as a continuum medium, k the Boltzman constant and T the absolute temperature. The Stokes expression for the friction coefficient holds in the case of a single particle diffusing in an infinite bulk liquid characterized by its viscosity η. When diffusion of the tracer occurs in an heterogeneous material – like porous media, gels or concentrated complex systems –, the diffusion is hindered by interactions, especially the long-range hydrodynamic interaction, of the tracer with the matrix structure.[19–23]

While the structure of glassy and glass-forming materials are spatially disordered,[3] such systems have been shown to be dynamically correlated on long time scales.[4,25] In this context, diffusion of tracers has been used to probe the dynamics of these materials, like in colloidal systems,[5,14] polymer networks,[26,27] as well as in glass-forming (supercooled) liquids.[28] Accordingly, tracers are usually chosen with the same size as the material constituents, as *e.g.* for the above-mentioned studies: molecular size in Refs.[26,28] and colloidal sizes (from 100 nm to 1 μm) in Refs.[5,27]

Although theoretical works suggest that the tracer characteristics dictate the way it couples to the soft glass and affect for instance the effective temperature it probes,[29] it appears that very little is known on the experimental side about how changing the tracer size modifies its diffusive motion in such systems. This is therefore the point on which we will more specifically focus in this study: we use a FRAP (Fluorescence Recovery After Photobleaching) technique to investigate the diffusive motion of tracers in a (colloidal) glass as a function of their size, covering probe

sizes ranging from molecular (1 nm) up to 100 nm. This range of scale allows us to probe the microscopic length scales of the Laponite suspension (platelet size and inter-distance), typically of the order of ten nanometers.

The paper is organized as follows. First, we discuss all experimental details in section , presenting the dedicated FRAP setup for measuring diffusion coefficients, and performing careful validations for diffusivity measurements in Laponite suspensions , regarding in particular aging effects and the sensitivity to Laponite preparation protocol. Then, we present the experimental results, i.e. the tracers diffusion coefficients in Laponite as a function of the probe size and Laponite concentration and analyze them in terms of Laponite structure and hindered diffusion in porous-like medium before concluding.

Materials and methods

Sample preparation

The investigated soft glassy material is a suspension of Laponite, that consists of disks of $\sim$30 nm diameter, 1 nm thickness, and 2.53 g cm^{-3} density, dispersed in aqueous solution.[30,31] The faces of these synthetic clay platelets of Laponite, with formula $Si_8[Mg_{5.5}Li_{0.4}O_{20}(OH)_4]^{0.7-}$ $Na_{0.7}^{0.7+}$, acquires a negative charge of roughly 1 e^{-1}.nm^{-2} (e charge of electron) upon solvation of Na^+ cations, while their edges are positively or negatively charged, depending on pH.[32–34] Solution are obtained by progressively adding the desired amount Laponite RD (Rockwood additives Ltd, used as received) to a dilution of fluorescent tracer particles in water, to obtain Laponite concentrations from 1 to 3.4%. The Laponite suspension self-buffers at pH 10, with an ionic strength of 2 to 8 mM[17] in the absence of any added salt. The obtained solution is stirred vigorously for 30 minutes to remove the initial turbidity and subsequently introduced in the optical cell and sealed with paraffin. The age of the Laponite system is calculated from this time on. A control vessel containing the same solution is kept to check the macroscopic gelation of the gel * . Typically the

*The term "gelation" is used in this paper to describe the macroscopic dynamical arrest of the structure.

gelation time ranges from a few minutes to a few months, and decreases with increasing Laponite concentration (see below).

Note that the range of available Laponite concentration is quite narrow. For mass fraction of 1%, i.e., 10 g L^{-1}, or less, the gelation time is generally too long and the Laponite solution is damaged before gelation (due in particular to the long time chemical detioration due to CO_2). For mass fraction of 4 %, i.e., 42 g L^{-1}, or more, gelation occurs before the stirring has dispersed the powder, therefore an inhomogeneous and cloudy gel is obtained.

As fluorescent probe particles, we used either fluorescein molecules, the hydrodynamical diameter of which is about 1 nm, or commercial polystyren fluorescent nanobeads with diameters ranging from 25 to 100 nm. We mention that finding fluorescent tracers with size smaller than 100 nm, suitable for working in Laponite suspension is a difficult task, as emphasized in Ref.[35] The stability of the colloidal tracers dispersed in water buffered at pH 10 was systematically tested. We only considered stables colloids with diffusion coefficients showing no significant variations on time scales comparable with Laponite suspension gelation time (see Section "Measurement of tracer diffusion in Laponite"). In a few situations (nanoH® fluorescent beads) the gelation of Laponite solution was observed to be prevented by the presence of the tracers, and those measurements were accordingly discarded. Altogether the different fluorescent probe particles used in this study are presented in Table 1. The reported sizes (1, 25, 37, 65 and 100 nm) have been determined through a FRAP measurement of their diffusive properties in pure water solutions. Initial colloidal solutions are diluted in ultrapure water (Milli-Q, Millipore) at concentration below 0.2% in volume which provided a satisfactory trade-off for FRAP measurements: low enough to remain bleachable without significant heating of the liquid, and high enough to lead to a good signal-to-noise ratio. Finally, the combination of small-sized particles and weak density mismatch (1.05 for polystyren spheres) prevented the occurence of sedimentation processes in the course of the experiments.

Table 1: Summary of fluorescent probe particles used. The actual size is deduced from FRAP measurements of the particles diffusion coefficient in water through Stokes-Einstein law. Colloids' manufacturers: $^{(a)}$, FluoProbes® ; $^{(b)}$ Polyscience®; $^{(c)}$, Kisker® ; $^{(d)}$, Molecular Probes®.

FRAP measured diameter σ (nm)	nominal diameter σ_n (nm)	diffusion coefficient $\mu m^2 s^{-1}$	standard error $\mu m^2 s^{-1}$
1	/	427	5
25 ± 0.5	$28^{(a)}$	17.5	0.3
37 ± 2	$50^{(b)}$	11.7	0.6
65 ± 7	$70^{(c)}$	6.7	0.7
100 ± 2	$100^{(d)}$	4.3	0.1

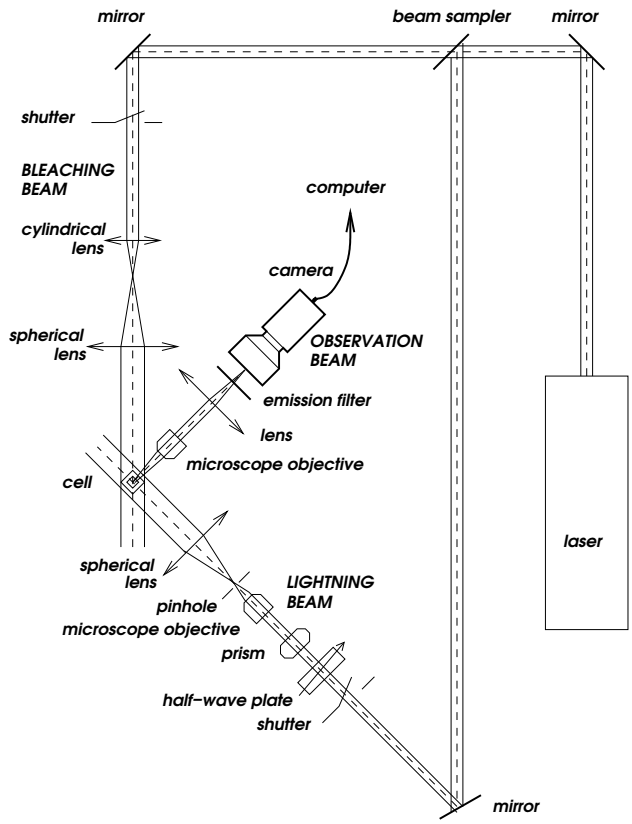

Figure 1: Fluorescence Recovery After Photobleaching setup (see text for details).

FRAP measurement setup

Diffusion coefficient measurements were carried out by means of a modified version of the Fluorescence Recovery After Photobleaching (FRAP) technique which has been widely used in biophysics in the study, for instance, of protein diffusion in phospholipid bilayers.[36] The general principle of the measurement is that an intense laser beam is used to photobleach the fluorescence of tracers in a small region of the sample. A much weaker beam then monitors the recovery of the fluorescence signal as unbleached tracers diffuse into the bleached area. In order to gain accuracy and robustness against possible artefacts, our implementation of the FRAP technique differs from the classical one of Axelrod *et al.*[36] where only the overall fluorescence signal of the bleached area is recorded. Adapting a previously proposed configuration,[37] we image here the imprinted photobleaching pattern as a function of time.

More precisely (see Figure 1), the 488 nm ray (2 Watts power) of an Ar^+ laser (Spectra-Physics) is divided into a photobleaching beam and an illuminating by a 90%/10% beam-splitter. The photobleaching beam passes through a cylindrical–spherical lens combination to generate a horizontal laser sheet having a vertical beam waist of 110 μm at the location of the sample cell. Illuminating beam is further attenuated by a half-wave plate combinated with a Glan-Taylor polarizer before passing through a spatial filter and being enlarged to provide uniform illumination at the scale of the observed sample region. The latter is monitored onto a cooled CCD Camera (CoolSnap HQ2, RoperScientific) through a microscope objective and lens tube (Plan Fluor x4, NA=0.13, Nikon) and an emission bandpass filter (545AF75, Omega). The whole setup is located on a vibration-damping table, while photobleaching and illuminating beam lines are controled by computer-driven shutters.

Depending on the fluorescent probe characteristics and concentration, and on the cell geometry, a photobleached layer is imprinted into the sample in a time ranging from 50 ms to 3 s (Figure 2a). The evolution of the photobleached layer is then followed through the intensity profile $I(z,t)$ along the vertical direction (perpendicular to bleached layer) extracted from camera images (Figure 2b). To improve accuracy, remaining inhomogeneities in the illuminating beam are corrected using a

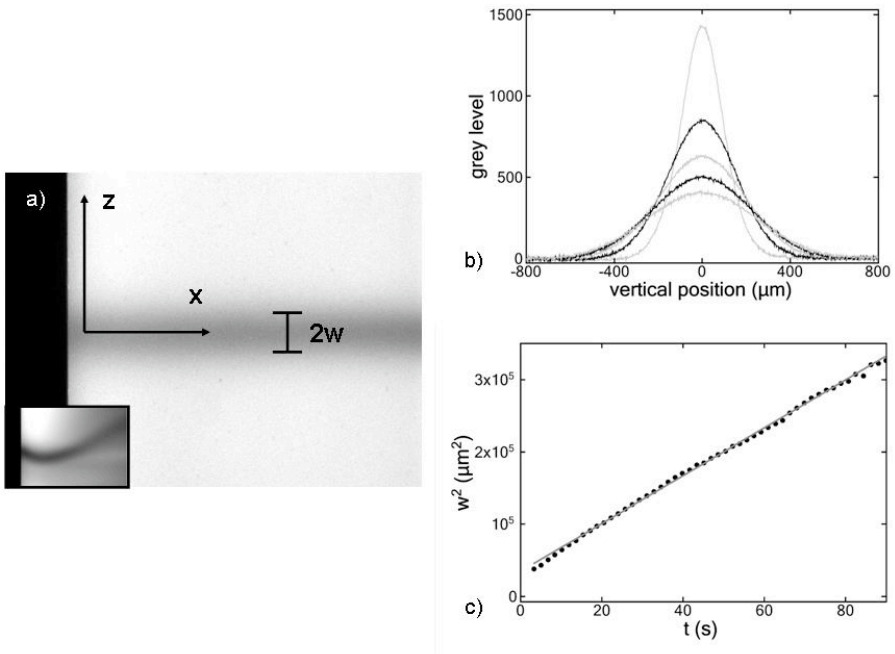

Figure 2: Evolution of a photobleached slab of solution. a) Typical image of the photobleached sheet (inset: sheet distorsion in presence of thermal convection); b) Fluorescence intensity profiles of fluorescein solution photobleached at $t = 0$, after various elapsed times (from 3 to 64 s); c) Time evolution of the squared width w^2 of the gaussian photobleached intensity profile during fluorescence recovery.

recorded image of the pre-bleached (homogeneously fluorescent) sample, and vertical intensity profiles are averaged in the x (horizontal) direction.

The initial fluorescent intensity profile of the imprinted layer just after photobleaching appears perfectly described by a gaussian profile $I(z,0) = I_0 \exp(-2z^2/w_0^2)$ and therefore remains gaussian throughout its evolution (Figure 2b) governed by 1-dimensional diffusion laws:

$$I(z,t) = I_0 \frac{w_0}{w(t)} \exp\left(-\frac{2z^2}{w(t)^2}\right) \tag{2}$$

where $w(t)$, the $1/e^2$ profile waist, obeys the classical relationship (Figure 2c)

$$w(t)^2/2 = 4Dt + w_0^2/2, \tag{3}$$

from which the diffusion coefficient of the fluorescent probe is obtained[†].

Compared with usual implementations of FRAP technique, imaging the photobleached area presents several advantages. First, the actual initial condition immediately after photobleaching is actually measured, and does not need being modeled. Second, the presence of hydrodynamic flows is readily detected, avoiding artefacts in analysis of the fluorescence intensity evolution. This is particularly important for FRAP experiments in low viscosity systems where thermal heating during photobleaching can give rise to convective instabilities. This was especially true with colloidal probes, the quantum yield of which was, according to the manufacturers, at most below 50%, getting much lower when the colloids size increases. This effect manifested itself directly on global distorsions of the photobleached horizontal layer resulting from non-zero velocity field, as can be seen in the inset of Figure 2(a). Such a convective effect is also evidenced on the squared width evolution, $w^2(t)$, which departs from a linear time behavior (not shown) as a consequence of the existence of a hydrodynamical flux replacing the diffusional migration of the fluorescent colloids.

In the following, special care was taken to avoid these thermo-convective effects, first by mini-

[†]The gaussian amplitude evolution can also be used to deduce diffusivity although less accurately due mostly to residual bleaching during the recovery process.

mizing the photobleaching time and power while keeping a good enough signal-to-noise ratio; and second by confining the liquid in narrow optical cells which helps stabilizing the system. Depending on the viscosity of the system, containers with sizes from 250 μm to 3 mm were used.

Overall, our setup provides a very good accuracy determining diffusion constants in water in the range (1 to 10^3 μm^2/s) with standard deviations on measurements of few percents.

Measurements of tracer diffusion in Laponite

Diffusion versus age

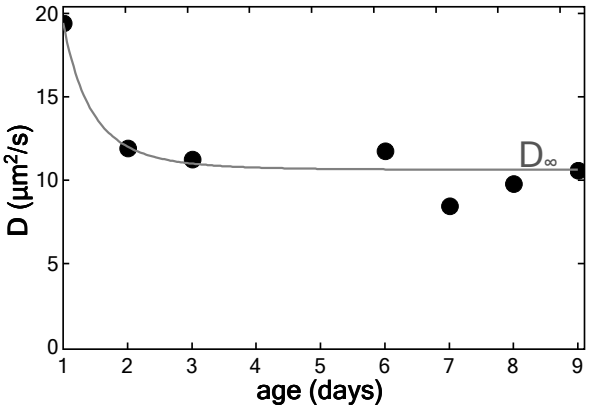

Figure 3: Typical time evolution of the diffusion coefficient of colloidal probe in laponite suspension (25 nm diameter colloids [see table Table 1] in $c = 1$ wt% laponite [nominal concentration]). The rather short gelation time measured for this low laponite concentration is probably due to the presence of surfactants conveyed by the added solution of fluorescent colloids.

The diffusion coefficients of the fluorescent tracers in the Laponite suspension were measured as a function of the time elapsed since cell filling. For all studied tracers and concentrations of Laponite, the time evolution of the diffusion coefficient presents first a decrease, due to the dynamical arrest process, before reaching a plateau after a "gelation time" t_g (see Figure 3). The dynamical arrest process, responsible for the gelation and aging dynamics of Laponite solutions, has been the object of numerous studies: t_g is known to increase when the Laponite concentration decreases, going here from less than a day for $c \geq 3$ wt%, to a few days for $c \simeq 2$wt% and up

to 20–60 days for $c \simeq 1$ wt%, values which are consistent with other studies[17,38,39] although the techniques of investigation are different. Indeed the reported values of t_g[40] demonstrate appreciable disparities in gelation time determinations. This can be explained partly by differences in definition depending on the performed experiments (dynamic light scattering[17,38,40] or rheological measurements[39–41]). Associated with this source of discrepancies, it is worth mentionning that the gelation process is also affected by small physico-chemical changes[17,39] and is therefore expected to be somewhat sensitive to the incorporation of tracers, even though at low concentration.

In the present paper, we therefore choose to concentrate on the behavior of the system past the initial evolution of the diffusion coefficient of the colloids, at times $t \gg t_g$. We report and discuss hereafter the dependency of the diffusion coefficient on the plateau D_∞ (see in Figure 3) as a function of the Laponite concentration and probe dimensions. We stress that D_∞ may also experience a slow evolution due to the ageing of the Laponite suspension. But this change occurs on timescales much greater than the ones investigated here and was not observed.

Independence of diffusion on experimental protocole

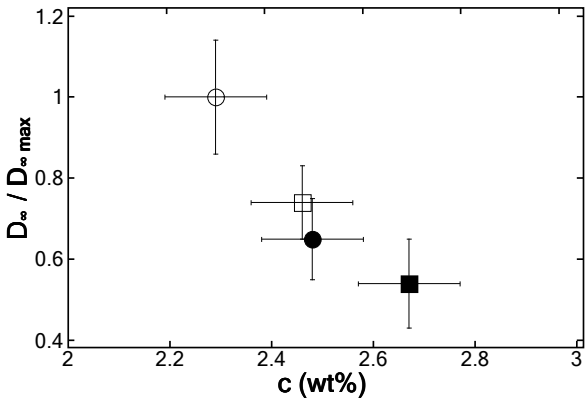

Figure 4: Diffusion coefficient of 37 nm diameter colloids as a function of the measured concentration of Laponite elaborated with different operating procedures (see text). The nominal concentration of Laponite is $c_n = 2.9$ wt% in the four cases.

In addition to gelation time, the phase diagram of the Laponite gel is known to be very sensitive

to small changes in the experimental conditions.[10,17,42] Before moving to experimental results, we therefore checked first the influence of the detailed procedure of Laponite preparation on the previously defined diffusion coefficient of the probes D_∞.

First of all, water readily adsorbs on Laponite clay and we therefore compared results obtained when the Laponite powder is either dried or not before its dispersion in water. Such a drying of the clay was achieved following the procedure used in Ref.:[10] the powder is heated in an oven at $T = 400$ K during four hours before being added to ultrapure water. In addition to water adsorption, filtration of the suspension also proved to be of primary importance when studying the light scattering signal from Laponite solutions.[43,44] We therefore also checked the effect of such a filtering on our probe diffusion measurements. When filtered, the suspension is pushed through a 0.45 μm filter to break up remaining aggregates.

Overall, a benchmark comparison was conducted on the probe diffusion properties for 4 different sample preparation procedures: (1) undried and unfiltered suspension, (2) undried and filtered suspension, (3) dried and unfiltered suspension, (4) dried and filtered suspension. In all cases a nominal laponite concentration of $c_n = 2.9$ wt% was achieved by dispersing the desired amount of the operated clay in ultrapure water.

Table 2: Influence of the sample preparation procedure on the actual laponite concentrations and on the diffusion coefficients D_∞ of 37 nm diameter colloids in the associated laponite gel. The diffusion coefficients are normalized by the diffusion coefficient $D_\infty^{(2)}$ measured with the procedure (2). The measured concentrations are normalized by the nominal sample concentration $c_n = 2.9$ wt%.

Operating procedure	Titrimetry	ICPAES	Titrimetry concentration ratio	FRAP diffusion ratio
	c (wt%)	c (wt%)	c/c_n	$D_\infty/D_\infty^{(2)}$
(1) undried/unfiltered laponite	2.52	2.57	0.87	0.74
(2) undried/filtered laponite	2.34	-	0.81	1
(3) dried/unfiltered laponite	2.74	-	0.95	0.54
(4) dried/filtered laponite	2.54	-	0.88	0.65

We first examine the actual Laponite concentration c resulting from the different sample preparations (see in Table 2), as determined from titrimetry and Induced Coupled Plasma Atomic Emis-

sion Spectroscopy (ICPAES). The principle of Laponite suspension titrimetry is described in details in:[42] it consists in dissolving Laponite at low pH before analyzing the concentration of dissolved Mg^{2+} by using complexiometric titrations[‡]. Starting with the effect of water absorption by Laponite powder, we note, comparing actual (c) and nominal (c_n) Laponite concentrations, that the undried clay retains 13% of water (protocol (1), table Table 2). This value is fully consistent with available results for water adsorption isotherms[45] showing that in standard conditions of temperature and humidity, Laponite adsorbs about 15% of water. The powder drying procedure indeed removes a significant part of the retained water but still shows a lower Laponite concentration ($c < c_n$, protocol (3), Table 2) associated with a remaining 5% water content –presumably due in part to water re-adsorption outside the oven. Finally, the effect of suspension filtering on the final laponite content is assessed by comparing protocols (1,2) or (3,4) in Table 2; overall it shows that about 7% of the initial amount is lost in the process, a value again consistent with the litterature where the effect of different filter sizes on light scattering measurements have been reported.[43]

Turning now to the diffusion properties of the same 37 nm colloidal probes in the differently prepared samples, it can be seen in Table 2 that D_∞ indeed varies with the preparation protocol. However, as can be clearly seen in Figure 4, such variations are merely related to the changes in the actual Laponite concentration and do not depend on the filtering itself –and the associated removal of platelet aggregates to which light scattering is sensitive– : the higher the actual concentration c of the prepared suspension, the lower the diffusion coefficient.

Provided the Laponite concentration is properly evaluated, the so-defined probe diffusion property thus appears well-defined and insensitive the details of sample preparations. In the following, all samples are prepared in the simplest way (undried/unfiltered) and Laponite concentrations c are measured independently using titrimetry. After these different experimental validations, we can now turn to the examination of the colloidal probes' dynamics in Laponite glasses.

[‡]More precisely, the concentration of Mg^{2+} is determined by titrating with ethylenediamine tetra-acetic acid (EDTA). The end of the titration is determined by the disappearance of the Mg^{2+}-eriochrome black T complex so by the suspension color change from red to blue.

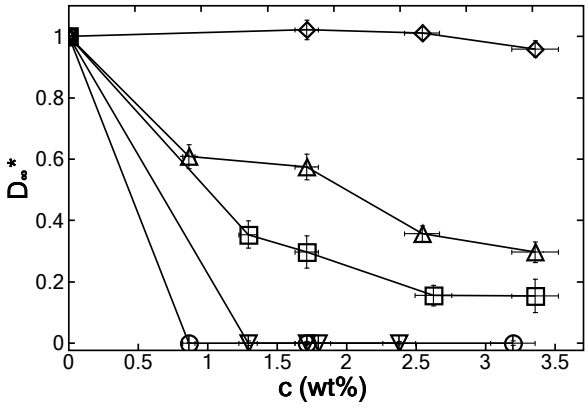

Figure 5: Evolution of the normalized diffusion coefficient, $D^*_\infty = D_\infty(c)/D_0$, of colloidal tracers in Laponite, as a function of the concentration of laponite for various tracer sizes: ($\Diamond$) 1 nm fluorescein molecules; ($\triangle$) 25 nm diameter colloids; ($\square$) 37 nm diameter colloids; ($\triangledown$) 65 nm diameter colloids; ($\circ$) 100 nm diameter colloids.

Probe size dependence of diffusion in Laponite

Diffusion coefficient of colloids in Laponite

We now examine the diffusive properties of colloidal tracer particles of various sizes, in order to probe Laponite suspension behavior and structure and capture some additional information on the local dynamical properties in this soft glassy material. Tracers characteristics were, for instance, theoretically predicted[29] to dictate the way the tracer couples to the soft glass thus affecting the effective temperature it probes. We therefore more specifically focus here on the role of the probed lengthscale, say σ in the Stokes-Einstein relationship in Eq. (1), on the measured diffusion coefficient D_∞. As already noticed, in a simple liquid the product $(D\sigma)$ should be constant (Eq. 1), whereas it is expected to vary in a glassy system if the size of the tracer approaches a characteristic length of the colloidal suspension.[27,28,35]

We report in Figure 5 the experimental diffusive properties of probes with sizes ranging from about 1 nm up to 100 nm (see Table 1) in Laponite glasses of various concentrations c. This figure displays, for the various tracers, the evolution of the probe diffusion coefficient in the Laponite glass, normalized by its measured value in pure water ($D^*_\infty = D_\infty(c)/D_0$), as a function of Laponite

concentration c. Each data point gathers the results of 10 to 100 independent measurements on different samples, from which the average value and standard deviation is obtained.

First, two extreme behaviors are readily observed. On the small size side, fluorescein molecules, with an hydrodynamic diameter around 1 nm, appear to keep a constant diffusion coefficient throughout the explored Laponite concentrations, thereby being totally unaffected by the presence of the Laponite disks in the glassy medium. On the large size side, at the opposite, the 65 and 100 nm diameter colloidal tracers are completely frozen in the Laponite glass, even for the lowest clay concentration we could investigate: $c \approx 1\%$. Their diffusivity therefore dropped to an extremely low value, below the sensitivity of our technique, in line with the high macroscopic viscosity of the Laponite glass under these conditions.[16,44]

Second, for intermediate probe sizes, corresponding here to 25 and 37 nm diameter colloids, the tracers diffusivity is lower than the one corresponding to the free solvent –water– dynamics, and gradually evolves toward a complete arrest ("gelled" medium) as the Laponite concentration increases. Comparing the evolution for the two different sizes, one evidences that the larger probe reaches the same D_∞^* (corresponding to the same reduction in diffusivity relative to the free solvent dynamics) for a lower Laponite concentration than the smaller one.

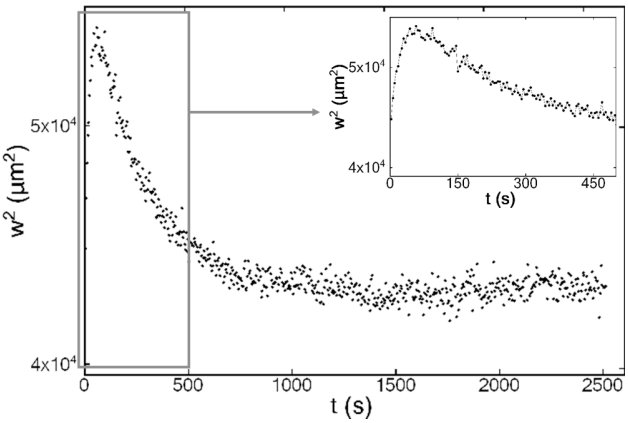

Figure 6: Non-monotonic evolution of the photobleached stripe width for a batch of bidisperse fluorescent colloids provided by Kisker ® in a Laponite glass of concentration 2.4 wt%. The insert shows the short time evolution of the waist diameter.

To better emphasize this size sensitivity of the probe slowing down, let us stress that 25 and 65

nm diameter colloids differ in normalized diffusion coefficient by more than 2 decades while only differing by less than a factor 3 in size. This result is similar to the enhancement in rotational diffusion of small molecules measured in ref.,[28] even though the investigated length scales are different in the two studies. As an illustration, we performed a test experiment using a Kisker nanosphere batch having a bimodal diameter distribution (with peaks given by the manufacturer at 26 and 75 nm). FRAP measurements performed in water (not shown) enabled to establish that the actual diameters were rather 25 and 65 nm. When dispersed in the same $c = 2.4$ wt% Laponite suspension, a complete separation in diffusion time scales is evident as shown in Figure 6. The effective photobleached width first increases due to 25 nm diameter colloids diffusion, with a dynamics agreeing with the one measured on monodisperse batch for a similar Laponite concentration (Figure 5). At larger times, only small colloids have homogeneized and the photobleached width is dominated by the 65 nm colloids signal. The latter appear completely frozen in the glass, with a diffusion dynamics orders of magnitude slower than expected from the simple size ratio, in agreement with the sieving effect already mentionned.

Hindered diffusion in the Laponite network

From the reported change of D_∞^* with size, it can be immediately inferred that a structural length around a few ten nanometers does exist in the Laponite glass. The exact structure of this material is still under discussion, but this characteristic length should be related in some manner to the average disk-to-disk distance d.

Consequently, the evolution of D_∞^* with the diameter σ of the probe can be interpreted in terms of a simple mechanism based on diffusion hindrance by the Laponite structure. Tiny probes essentially migrate in the inter-disks free solvent without feeling the platelets network, therefore showing an unaltered diffusion coefficient. As the probes become larger, they eventually experience motion hindrance by the surrounding Laponite disks that gets more and more pronounced as their size increases, in analogy to diffusion in a porous medium. Finally, when the probes are large enough that σ reaches a value of the order of the distance between Laponite particles, the hindrance is

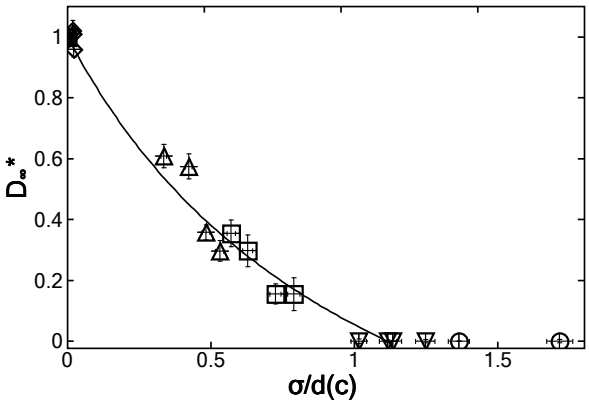

Figure 7: Normalized diffusion coefficient D^*_∞ as a function of the ratio between the probe size σ and the disk-to-disk distance $d(c)$ (see text): ($\Diamond$) 1 nm fluorescein molecules; ($\triangle$) 25 nm diameter colloids; ($\square$) 37 nm diameter colloids; ($\triangledown$) 65 nm diameter colloids; ($\circ$) 100 nm diameter colloids; (—) theoretical prediction from Eq. 5 with $C = 0.9$.

such that they appear embedded in the disks network therefore experiencing an extremely viscous environment and no detectable diffusion.

In this context, we thus expect that the measured decrease of diffusion coefficient D^*_∞ with the increase of Laponite concentration c should be directly related to the concomitant decrease of the disk-to-disk characteristic distance d. From a purely geometrical point of view, and *assuming a homogeneous spatial distribution of Laponite particles*, this suggests $d \propto c^{-1/3}$. More quantitatively, one expects $d = (6/\pi)^{1/3}(\rho_{\rm lap} v/\rho_{\rm glass})^{1/3} c^{-1/3}$ with c Laponite mass concentration, ρ_{lap}, ρ_{glass} the density of the Laponite disks and of the Laponite solution[§], and v the volume of a Laponite disk. In Figure 7, all experimental data for the normalized probes diffusivity D^*_∞ are plotted as a function of the ratio between the probes diameter and the above estimate of the mean disk-to-disk distance $\sigma/d(c)$. Interestingly, these simple "geometrical confinement" considerations do quite satisfactorily account for the various data sets, that gather to form a continuous evolution –although a definite evidence of a true master curve would require more overlap among the various data sets. In accordance with previous reasoning, the tracer diffusion is seen to become undetectable within

[§]Due to the presence of water, the Laponite glass density only depends slightly on c. For $c \leq 3.5\%$ wt, this dependence can be neglected as $\rho_{\rm glass}$ and $\rho_{\rm water}$ differ from less than 2%.

our experimental resolution when their size reaches the Laponite disk-to-disk distance: $\sigma \sim d(c)$.

Going further, the dependence of diffusion on geometrical parameters, σ and $d(c)$, suggests that the diffusion hindrance can be interpreted in terms of the hydrodynamic interactions between the probe and the Laponite disks structure, and not by their physico-chemical interaction. Accordingly the mechanism of probe diffusion in the Laponite glass is similar to that of hindered diffusion in an open porous network.[19,20]

Due to the long-range nature of hydrodynamic interaction, the description of diffusion processes in static (or dynamic) networks is in general a formidable task. We point for example to Refs.[22,23] for recent works on the diffusion of tracers in rod networks. In the present case, our measurements were performed after gelation occured and one may thus consider the laponite network as static for the tracer diffusion. Accordingly we do not consider the influence of ageing of the laponite structure at very long times: this should result in a small, long-time diffusion of the largest probes, which is not measured with the present experimental setup (see discussion below). Furthermore, the laponite network is made of an arrangement of disks and to our knowledge tracer diffusion in such a network has not been considered theoretically. Yet, we thus propose a simplified approach, aiming at rationalizing our experimental results.

In the limit where the probe size is small compared to the disk-to-disk distance, $\sigma \ll d$, the long-ranged hydrodynamic interactions can be expanded in powers of σ/d, thus leading to a probe diffusion coefficient behaving as:[20,46]

$$\frac{D}{D_0} = 1 - \alpha\frac{\sigma}{d} + \beta\left(\frac{\sigma}{d}\right)^2 + \ldots \tag{4}$$

with α, β numerical coefficients ($\alpha > 0$). In general, the expansion organizes itself as a multipole expansion of the hydrodynamic interactions between the probe and the structure.

Of course, such an expansion is expected to break down as the size of the probe reaches a fraction of the interparticle distance, $\sigma \sim d$: this is the dense regime. For laponite disks with diameter 30nm, this corresponds also to the situation where the probe size is of the same order as

the laponite disk size. In this limit, the probe's motion is strongly confined between the disks of the Laponite netword and the hydrodynamic interactions are strongly screened. But one may note that in this regime, probe diffusion should involve mainly motion of the beads parallel to the laponite disks, at a distance to the disk fixed by a fraction of d (since motion perpendicular to the disks is even more strongly hindered[46]). Under a drastic simplification, we propose accordinly to reduce the probe diffusive dynamics to this elementary process, *i.e.* involving motion parallel to laponite disks.

The mobility of a sphere moving parallel to a plane has been considered by Brenner,[46] and more recently in Refs.[47–49] in the context of diffusion in strongly confined geometry. An expression for the parallel diffusion coefficient between two walls separated by a distance d has been obtained in this geometry[46–49] and reads

$$\frac{D_{\parallel}}{D_0} = \frac{1}{\frac{2}{1-C\frac{\sigma}{d}} - 1} \tag{5}$$

with C a numerical constant ($C = 9/8$ for diffusion between two infinite rigid walls). This equation was shown to provide a good approximation for the diffusion processes down to strong confinement.[49] Here a limit is also provided by the condition $\sigma < d/C$. For larger d, a vanishing diffusion coefficient is expected. This expression should be merely considered as an interpolation between a strongly hindered regime, with $\sigma \sim d$ and $D \to 0$, and the dilute regime, with $\sigma \ll d$, in which the diffusion coefficients expands in σ/d along Eq.(4).

Nonetheless, it provides a useful fit for the evolution of the diffusion coefficient with σ/d: as is shown in Figure 7, the experimental results show good agreement with the fitting formula, Eq. (5), with $C = 0.9$.

Let us conclude this part by a few remarks:

First, as noted above, we have considered a "frozen" Laponite structure while in fact the diffusion motion of the probe inside the Laponite glass may be able to induce a local deformation of the structure. Indeed due to the soft nature of the Laponite glass, the clay platelets could be able

to rotate or move a small distance to make the probe migration easier. For instance, the time needed for the intermediate 37 nm probe, diffusing in 2 wt% Laponite, to move over a clay particle diameter is about 10^{-4} s. This is to compare with the characteristic time of the free diffusion of Laponite, i.e., the relaxation time of the rattling motion of a platelet in the cage formed by its neighbors, which has been evaluated by dynamic light scattering to be $\sim 10^{-4}$ s.[10,40] Consequently, the Laponite network may reorganize *locally* during the passage of a nanosphere and potentially facilitate its diffusion.

Second, an interesting remark is that the simple relationship $d(c) \propto c^{-1/3}$ provides a sound estimate of the disk-to-disk distance characterizing the diffusive dynamics insider the Laponite glass structure. This promotes the idea that the spatial distribution of the platelets is homogeneous, although a definite proof of this homogeneous structure has not been reached up to now in the litterature. Using the distinction between a colloidal gel and a colloidal glass given in ref.,[16] our result is in favor of a glass whose characteristic length scale is of the order of the inter-particle distance whereas the characteristic length scale of a gel would be expected to be much larger than the size of its constitutive colloids.

Finally, it is interesting to mention that the above evolution of $D(\sigma)$ can be alternatively interpreted by considering that the colloids migrate in an inhomogeneous medium showing a scale-dependent effective viscosity $\eta_{\text{eff}}(\sigma)$. This interpretation has been proposed in a different context for the scale dependent viscosity of polymers melts,[50] as well as in recent experiments on diffusion in crowded micellar solutions[24].

In the present case, this viscosity can be estimated using a Stokes-Einstein type relation, thus defining a viscosity $\eta_{\text{eff}}(\sigma) = kT/(3\pi\sigma D(\sigma))$. The extreme values of $\eta_{\text{eff}}(\sigma)$ are known: in the limit where the colloids are so small that they diffuse freely in the Laponite structure then $\lim_{\sigma\to 0} \eta_{\text{eff}}(\sigma) = \eta_{\text{water}}$; in the opposite limit where the colloids are large compared to the Laponite structure, they feel the macroscopic viscosity of the Laponite glass and $\lim_{\sigma\to\infty} \eta_{\text{eff}}(\sigma) = \eta_{\text{macro}}$ ($\gg \eta_{\text{water}}$). Typically, η_{macro} is five to six orders of magnitude higher than the water viscosity.[16,44] For intermediate scales, the scale dependent viscosity will interpolate between these extreme values.

Assuming $\eta_{\text{macro}} = \infty$, Eq. 5 provides an empirical expression for the scale dependent viscosity, in the form $\eta_{\text{eff}}(\sigma) = \eta_{\text{water}} \left[2(1 - C\sigma/d)^{-1} - 1\right]$, for $\sigma < d/C$, while $\eta_{\text{eff}} = \infty$ for $\sigma > d/C$.

Conclusion

In the present work, we have used a modified Fluorescence Recovery After Photobleaching setup to measure the diffusion coefficient of fluorescent nanoprobes, of sizes ranging between 1 and 100 nm, in Laponite glasses of concentrations from 1 to 3.4 wt%. A change of diffusive behavior is evidenced for probe sizes around a few ten nanometers, which corresponds to the typical distance between the disk of clay constituting the soft glass skeleton. Far below this value, the nanospheres migrate in the solvent showing little interaction with the Laponite, and their diffusion coefficient is the same as in pure solvent. Far above this value, the motion of the nanospheres is strongly hindered by the network of Laponite platelets and their diffusion coefficient is seen to vanish. In between, increasing the probe size leads to a gradual increase of the hindrance of diffusive motion by Laponite platelets from free solvent diffusion down to experimentally undetectable motion. The diffusion coefficient measured for various probe sizes and Laponite concentrations are shown to be well accounted for when considering only a dependency on probe size to disk-to-disk distance ratio. This simple dependence promotes the picture of a homogeneous glass structure characterized by a well defined interparticle distance, and indicates that the hindered diffusion originates in the hydrodynamic interaction between the probe and the Laponite glass structure. In particular, it shows that in such situation the relationship between diffusivity and probe size results from the heterogeneous nature of the soft glass at the scale of the probe, which can be accounted for by a scale dependent viscosity in line with results for polymers.[50]

Acknowledgements— We thank Jean-Louis Barrat for many interesting discussions and suggestions. We acknowledge support from the ANR, through the program 'ANR Blanche' (Sllocdyn).

References

(1) J.R. Stokes and W. J. Frith, *Soft Matter* **4** 1133 (2008).

(2) P. Coussot, *Soft Matter* **3** 528 (2007).

(3) G. Biroli, *Nature Physics* **3**, 222 (2007).

(4) L. Berthier, G. Biroli, J.-P. Bouchaud, L. Cipelletti, D. El Masri, D. L'Hôte, F. Ladieu, M. Pierno, *Science* **310**, 1797-1800 (2005).

(5) E. Weeks and D. Weitz, *Phys. Rev. Lett.*, vol. 89, p. 095704, 2002.

(6) F. Varnik, L. Bocquet, J.-L. Barrat, L. Berthier, *Phys. Rev. Lett.* **90**, 095702 (2003).

(7) Isa, L., Besseling, R., Poon, W.C., *Phys. Rev. Lett.* **98**, 198305 (2007).

(8) J. Goyon, A. Colin, G. Ovarlez, A. Ajdari, L. Bocquet, *Nature* **454**, 84-87 (2008)

(9) A. Knaebel, M. Bellour, J. Munch, V. Viasnoff, F. Lequeux, and J. Harden, *Europhys. Lett.*, vol. 52, p. 73, 2000.

(10) B. Ruzicka, L. Zulian, and G. Ruocco, *Phys. Rev. Lett.*, vol. 93, p. 258301, 2004.

(11) B. Abou and F. Gallet, *Phys. Rev. Lett.*, vol. 93, p. 160603, 2004.

(12) L. Bellon, S. Ciliberto, and C. Laroche, *Europhys. Lett.*, vol. 53, p. 511, 2001.

(13) S. Jabbari-Farouji, D. Mizuno, M. Atakhorrami, F. C. MacKintosh, C. F. Schmidt, E. Eiser, G. H. Wegdam, and D. Bonn, *Phys. Rev. Lett.*, vol. 98, p. 108302, 2007.

(14) D. Strachan, G. Kalur, and S. Raghavan, *Phys. rev. E*, vol. 73, p. 041509, 2006.

(15) P. Jop, J. Ruben Gomez-Solano, A. Petrosyan and S. Ciliberto, *Submitted to J. Stat. Mech.*, ArXiv:0812.1391, 2009.

(16) H. Tanaka, J. Meunier, and D. Bonn, *Phys. Rev. E*, vol. 69, p. 031404, 2004.

(17) P. Mongondry, J. Tassin, and T. Nicolai,*J. Colloid Interf. Sci.*, vol. 283, p. 397, 2005.

(18) S. Jabbari-Farouji, G. H. Wegdam, D. Bonn, *Phys. Rev. Lett.* **99**, 065701 (2007).

(19) A. Pluen, P.A. Netti, R. K. Jain, D. A. Berk, *BioPhys. J.* **77** 542-552 (1999)

(20) R.J. Phillips, *BioPhys. J.* **79** 3350-3354 (2000)

(21) S. Babu, J.-C. Gimel, T. Nicolai, *J. Phys. Chem. B* **112** 743-748 (2008)

(22) K. Kang, *et al. J. Chem. Phys.* **122**, 044905 (2005)

(23) K. Kang, A. Wilk, A. Patkowski, J.K.G. Dhont *J. Chem. Phys.* **126**, 214501 (2007)

(24) J. Szymanski, A. Patkowski, A. Wilk, P. Garstecki, and R.. Holyst *J. Phys. Chem. B* **110** 25593 (2006).

(25) Y. Gao, M.L. Kilfoil, *Phys. Rev. Lett.* **99**, 078301 (2007).

(26) A. Ekani-Nkodo and D. Fygenson, *Phys. Rev. E*, vol. 67, p. 021909, 2003.

(27) I. Wong, M. Gardel, D. R. E. Weeks, N. Valentine, A. Bausch, and D. Weitz, *Phys. Rev. Lett.*, vol. 92, p. 178101, 2004.

(28) M. Cicerone and M. Ediger, *J. Chem. Phys.*, vol. 104, p. 7210, 1996.

(29) L. Berthier, J.-L. Barrat, *J. Chem. Phys.* **116** 6228 (2002).

(30) R. Avery and J. Ramsay, *J. Colloid Interf. Sci.*, vol. 109, p. 448 (1986).

(31) M. Kroon, W. Vos, and G. Wegdam, *Phys. Rev. E*, vol. 57, p. 1962 (1998).

(32) H. V. Olphen, *An introduction to clay colloid chemistry*. wiley ed., 1977.

(33) D.W. Thompson and J.T. Butterworth, *J. Colloid. Interface Sc.*, **151**, 236 (1992)

(34) H. Zhao, S. Bhattacharjee, R. Chow, D. Wallace, J. H. Masliyah, Z. Xu, *Langmuir*, **24** 12899 (2008).

(35) T. Waigh, *Rep. Prog. Phys.*, vol. 68, p. 685 (2005).

(36) D. Axelrod, E. Koppel, J. Schlessinger, E.L. Nelson, W.W. Webb, *BioPhys. J.* **16** 1055 (1976)

(37) J. Bechhoefer, J.-C. Géminard, L. Bocquet, P. Oswald, *Phys. Rev. Lett.* **79** 4922-4925 (1997)

(38) M. Kroon, G. Wegdam, and R. Spirk,*Phys. Rev. E*, vol. 54, p. 6541, 1996.

(39) S. Cocard, T. Nicolai, and J. Tassin, *J. Rheol.*, vol. 44, p. 585, 2000.

(40) T. Nicolai and S. Cocard,*J. Colloid Interf. Sci.*, vol. 244, p. 51, 2001.

(41) J. Ramsay, *J. Colloid Interf. Sci.*, vol. 109, p. 441, 1986.

(42) A. Mourchid and P. Levitz, *Phys. Rev. E*, vol. 57, p. R4887, 1998.

(43) L. Rosta and H. von Gunten, *J. Colloid Interf. Sci.*, vol. 134, p. 397, 1990.

(44) D. Bonn, H. Kellay, H. Tanaka, G. Wegdam, and J. Meunier, *Langmuir*, vol. 15, p. 7534, 1999.

(45) P. Kaviratna, T. Pinnavaia, and P. Schroeder, *J. Phys. Chem Solids*, vol. 57, p. 1897, 1996.

(46) J. Happel and H. Brenner, *Low Reynolds number hydrodynamics*. Kluwer, 1984.

(47) L. Joly, *Nanohydrodynamique au voisinage d'une surface solide : de la caractérisation expérimentale à l'équilibre aux conséquences sur la dynamique des systèmes chargés*. PhD thesis, University of Lyon I, FRANCE, 2005, p71.

(48) L. Joly, C. Ybert, and L. Bocquet, *Phys. Rev. Lett.*, vol. 96, p. 046101, 2006.

(49) A. Saugey, L. Joly, C. Ybert, J.-L. Barrat, L. Bocquet, *J. Phys. : Cond. Matt.* **17** S4075 (2005).

(50) F. Brochard-Wyart and P.G. de Gennes *Eur. Phys. J. E* **1** 93 (2000).

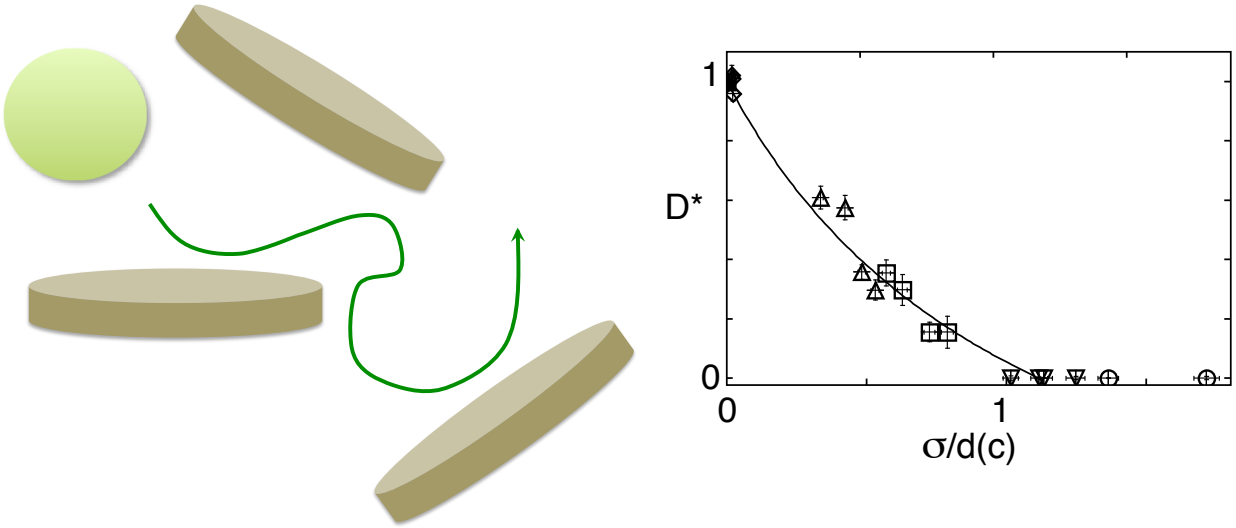

Figure 8: Graphic for TOC